

Modeling of pH Distribution Over Corrosion Sites

Maher A. Alodan

*Department of Chemical Engineering, King Saud University
P.O. Box 800, Riyadh 11421, Saudi Arabia
alodan@ksu.edu.sa*

(Received 07 July, 2001; accepted for publication 03 November, 2001)

Abstract. Different corrosion reactions were studied as a function of the bulk electrolyte pH, acidic, neutral and alkaline pH. Three variables, H^+ , OH^- and dissolved metal ions concentration were modeled along with the water ionization reaction as a homogeneous reaction. Different geometries were selected to simulate metal corrosion around inclusions, similar to Al and steel alloys corrosion. Modeling showed that reduction of O_2 at an inclusion caused the pH to increase at and around the inclusion. Coupling the reaction to dissolution of the surrounding metal matrix showed that the pH was decreased over the anodic dissolution region. The pH distribution was strongly affected by the bulk pH and was confined to 50 μm distance from the surface. Metal ions concentration was found to be affected mostly by the system geometry.

Key Words: *Heterogeneous Reactions, Finite Element, Aluminum Alloys Corrosion, Inclusions.*

Introduction

Corrosion reactions occur on most metal surfaces with different rates depending on the nature of the metal, environment and temperature. Most of active metal surfaces react to the corrosive environment in a non-uniform manner, i.e. heterogeneous reaction. The oxidation, or anodic, reaction occurs on one area while the reduction, cathodic, reaction occurs on another area or location. Nevertheless, the distance between the two reactions is relatively small distance to minimize ohmic losses. Several factors may contribute to the separation of the anodic and cathodic reactions, such as the nature of the oxide layer, surface and bulk defects, and concentration variations over the corroding surface [1, p. 64, and 2, p. 212]. Accordingly, different local environments may exist over the anode and the cathode and manifest themselves as variations in pH, cations or/and anions concentration, and formation of corrosion products.

Most common cathodic reaction in aqueous systems is the reduction of dissolved oxygen to form hydroxyl ions in neutral or alkaline media or to form water molecules in acidic media. Anodic reactions vary according to the corroding metal. In general, metals

are oxidized to form metal cations, which might react further (hydrolyze) with water to form hydrogen ions [2,3]. Several corrosion systems behave in similar manner to the above mechanism such as Al2024, Al6061, and steel. In these systems, metallurgical inclusions serve as cathodic sites for the reduction of oxygen. For example, it is known that oxygen is reduced on copper rich inclusions in Al2024 alloys, and this reaction is coupled to the anodic reaction on or around the individual inclusions [4,5]. The anodic reactions may include metal dissolution from the surrounding matrix. The reduction of oxygen causes the local pH to increase over an inclusion unless it is balanced locally by anodic dissolution and hydrolysis reactions. Increased alkalinity has been proposed to extend over the surrounding metal matrix [3] if the matrix in that region is electrochemically inactive. On the other hand, the anodic dissolution of the matrix may be enhanced around the periphery of the inclusion particles so that grooves are created that may allow to eventually undermine the encircled particle.

Recently, aluminum alloys, Al2024 and Al6061, were studied and it was found that the fluorescent dye fluorescein decorated inclusion sites so that the sites could be seen by using confocal laser scanning microscopy (CLSM) [5,6,7]. The inclusion sites were confirmed to be cathodic sites depending on the chemical constituents of the inclusions. Several different types of inclusions were found on Al alloys, and there were some differences in the fluorescent pattern that was seen on the different inclusion types as well. Based on chemical constituents, Al6061 had two types [5] of inclusions and four types of inclusions were found [7] on Al2024 surfaces as determined by scanning electron microscopy/energy dispersive x-ray analysis (SEM/EDX). It is clear from previous studies of fluorescence microscopy and other observations that the specific reactions that occur at inclusions on aluminum alloy surfaces, as well as their distribution, are different at inclusions of different types. The previous described work suggests the importance to model such systems to understand the distribution of pH and other ions involved in the corrosion reaction.

Several modeling and simulation studies have been carried out to understand and evaluate corrosion systems. Pitting behavior of iron systems has been modeled and analytical solutions have been developed based on concentration and potential variation in the pit [8]. A similar system of galvanic cells was treated with finite difference techniques to solve for potential and current distribution [9]. Simulation of crevice and pitting corrosion was carried out using the orthogonal collocation method and comparison with different computational techniques was presented [10]. In addition to the interest in evaluating the current and potential distribution for the coupled reactions, it is clear that it is important to take into account the concentration distributions of important species as well. In the present paper, finite element calculations was used to model the concentration distribution of hydrogen ions (pH) and other species on and around inclusions on steel alloy surfaces.

Mathematical Model

The main geometry of the modeled system is shown in Figure 1. The cathode, or the inclusion in the case of aluminum alloy, represents a 10 μm disk surrounded by the anodic plane. Different diameters of the anodic plane were used (10, 50, and 100 μm). The anodic plane is also surrounded by an infinite inert plane to limit ohmic losses and to simulate bulk infinite conditions. Similar corrosion geometry was found and observed for steel and Al alloys as discussed earlier.

The main cathodic reaction studied is the reduction of oxygen on the cathode and two types of anodic reactions were considered. The first type is the dissolution of the metal ions and further hydrolyze reaction to produce hydrogen ions. The second reaction is the oxidation of metal ions in acidic environment to produce cations. The two reactions were investigated according to the bulk pH, acidic and neutral and alkaline which both have their importance in industrial processes.

The dissolved oxygen concentration in water at 25°C and one atmosphere pressure (air) is 0.267 mM [11] and is nearly independent of electrolyte composition at low concentrations of the latter. Reduction of oxygen at a small disk has been treated mathematically and experimentally [12,13] and it was found that steady state of oxygen concentration is reached within one second for 10 micrometer disk diameter according to Cottrell's equation [13]. The resulting limiting reduction current of oxygen was found to be 50 $\mu\text{A}/\text{cm}^2$ [12]. In the present work, steady state conditions were modeled since time transients are very short as demonstrated by previous work [12]. The model was solved by finite element software from FEMLAB by COMSOL. The software is capable of solving partial differential equations with several independent variables with either linear or nonlinear coefficients.

1) Neutral and alkaline solutions

In neutral and alkaline environment, oxygen reduction can be assumed to be uniform over the disk and can be written as:



The concentration gradient of OH^- at the disk surface is connected to the rate of reduction of O_2 and can be written as the following:

$$\frac{\partial C_{\text{OH}^-}}{\partial z} = \frac{i_o}{F D_{\text{OH}^-}} \quad (2)$$

Where i_o is limiting current of oxygen reduction, D_{OH^-} is the hydroxyl ion diffusion coefficient, F is Faraday number.

The anodic reaction on passivating metals (e.g., Al and iron) is the dissolution of metal and further hydrolyze of the metal ions to produce hydrogen ions. In the case of iron the anodic reaction can be written as [2, p. 21]:



The formation of the passive film depends on the local pH and can be sustained in relatively moderate pH levels, between 6 and 10. In our discussion, early stages of corrosion was studied rather than long term exposure where the passive film starts to interfere with the reduction reaction and change the reaction rate.

From equation (3), the concentration gradient of H^+ ions over the surrounding metal matrix can be expressed as:

$$\frac{\partial C_{\text{H}^+}}{\partial z} = \frac{i_o}{FD_{\text{H}^+}} \left(\frac{A_{\text{cathode}}}{A_{\text{anode}}} \right) \quad (4)$$

Here, D_{H^+} is the diffusion coefficient of hydrogen ions and A_{cathode} and A_{anode} are the areas of the cathode (disk) and anode (annulus), respectively. The oxidation and reduction reactions are linked through electroneutrality conditions, i.e., the total production rate of OH^- is equal to that of H^+ .

2) Acidic solutions

In acidic solutions the reduction of oxygen is:



The concentration gradient of H^+ at the surface is determined by the reduction current according to the following equation:

$$\frac{\partial C_{\text{H}^+}}{\partial z} = - \frac{i_o}{FD_{\text{H}^+}} \quad (6)$$

The minus sign before the right hand side indicates consumption of hydrogen ions. The anodic reaction on the surrounding matrix involved the direct dissolution of the metal ions which is valid reaction for most metals in acidic environment; below pH 4. The reaction can be written as the following:



The gradient of the metal ions at the surface can be expressed as function of the reduction current in similar manner to equation (4) but for ferrous ions:

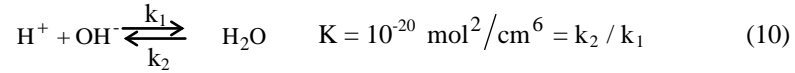
$$\frac{\partial C_{\text{Fe}^{2+}}}{\partial z} = \frac{i_o}{FD_{\text{Fe}^{2+}}} \left(\frac{A_{\text{cathode}}}{A_{\text{anode}}} \right) \quad (8)$$

In acidic solutions, there are neither production nor consumption of hydrogen and hydroxyl ions on the anode.

In the solution domain, the electrolyte concentration is KCl (0.1 M) which is much larger than that of H^+ or OH^- for all the examples treated in the present work. Since the total corrosion current is small, the effect of migration on the species fluxes was considered to be small compared to that of diffusion. Therefore one can neglect the effect of migration which is reasonable assumption in this case, and the conservation of mass for H^+ and OH^- at steady state in stagnant solutions [14] is expressed as:

$$D_i \nabla^2 C_i + R_i = 0, \quad i = \text{H}^+ \text{ or } \text{OH}^- \quad (9)$$

The Laplacian operator in equation (9) is for two-dimensional cylindrical coordinates centered over the disk. It was assumed that the concentrations were independent of the angle of rotation around the z-axis. R_i term in equation (9) represents source term, which is any homogeneous chemical reactions in solution. In the case of aqueous electrolytes, the ionization-dissociation of water represent an important reaction during local pH variation, the reaction can be written as



The equilibrium in equation (10) is often overlooked in modeling calculations, but it is the dominating reaction for distributions that involve hydrogen ions and hydroxide ions. The homogeneous production rate of the two ions, R_i , is associated with the dissociation of water and can be expressed as

$$R_i = k_2 - k_1 (C_{\text{H}^+} C_{\text{OH}^-}) = k_1 (K - C_{\text{H}^+} C_{\text{OH}^-}) \quad (11)$$

Here, k_2 and k_1 are the forward and backward rate constants for reaction (10) as written. The value of k_1 is $1.4 \times 10^{14} \text{ (cm}^3/\text{mol.s)}$ [15] and K is 10^{-20} in units of mol^2/cm^6 [16]. Similar equation to (9) can be written for metal ions but without source term, in the case of acidic solution, as the following

$$\nabla^2 C_{\text{Fe}^{2+}} = 0 \quad (12)$$

As mentioned earlier, it was found that the time to reach steady state conditions is very short and it was calculated to be within one second. This finding justifies the steady assumption of equations (9) and (12).

Different radii of the anodic plane, 20, 50, and 100 μm , were investigated to understand the effect of area ratio between the anode and cathode. Also, different bulk pH were studied to simulate different solution conditions and to understand the effect of metal passivation or active dissolution.

In neutral and alkaline conditions, pH 7 and pH 10, equation (9) was solved for hydrogen ions and hydroxyl ions, since these ions are the only product from the surface. Equations (2) and (4) were used as boundary conditions for OH^- and H^+ ions, respectively. On plane 1 and 2 the fluxes of the ions were zero because of symmetry conditions. On plane 3, bulk concentration values were used in the model. Fluxes of all ions were zero on the inert plane 4 (see Fig. 1).

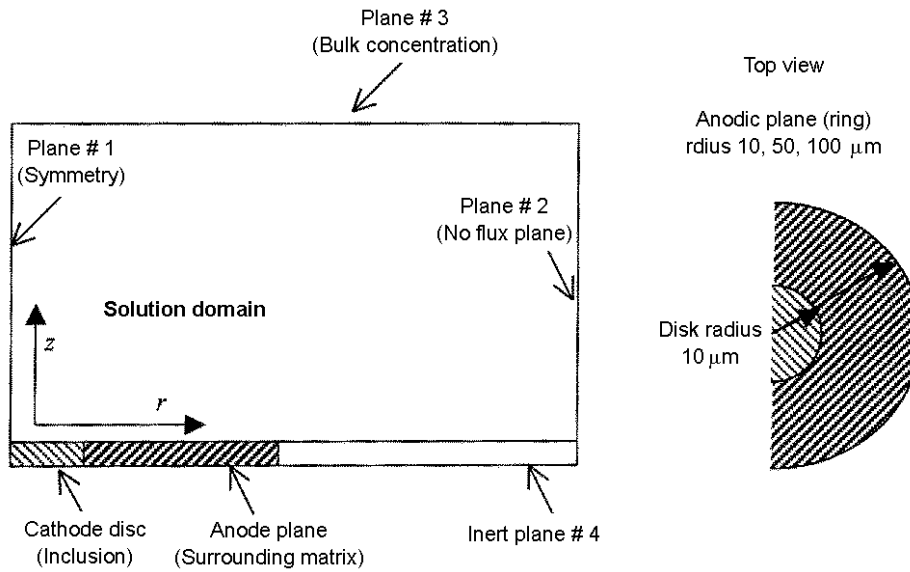


Fig. 1. A schematic diagram indicating the geometry of the model. Left, is a side view of the solution domain, Right, is top view of the surface, (different scale).

In acidic environment, Equation (9) was solved for OH^- and H^+ ions and equation (6) was used as a boundary condition for H^+ ions. The OH^- flux was zero on the cathode and the anode as well. Similar boundary conditions were used for the other planes as in the alkaline case. Equation (12) was solved for the ferrous ions to obtain the ferrous ions concentration distribution in acidic environments.

The dimension of the total domain was $200\mu\text{m}$ by $200\mu\text{m}$ or 20 disk radius units to ensure bulk conditions. The finite element grid distribution is shown in Fig. 2. Fine grid size was chosen near sharp changes to maintain solution accuracy.

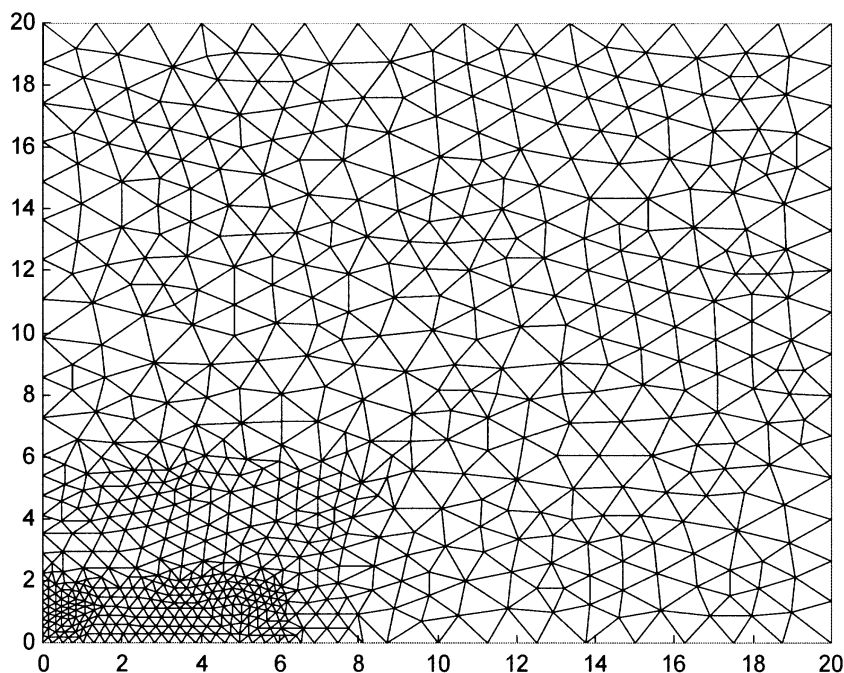


Fig. 2. Finite elements grid distribution in the solution domain, finer grid near sharp changes is selected in the solution to maintain accuracy.

Results and Discussion

Concentration and pH profiles as function of the different anode geometries and bulk pH were solved and results are presented and discussed in this section. Fig. 3 shows the normalized pH distribution around the disk-ring for a bulk pH of 4, 7, and 10 for a disk radius of 10 μm and an outer ring radius of 50 μm . The pH values were reported as normalized values to the bulk pH for comparison between the different bulk values. The results were similar to the values reported previously [5] where the outer ring radius was 20 μm . It can be seen from Figure 3 that an alkaline condition was generated over the disk where O_2 is cathodically reduced, but the pH was reduced on the nearby ring where anodic dissolution of iron and production of ferrous hydroxide species, $\text{Fe}(\text{OH})_2$, was assumed. Decreasing the ring diameter from 50 to 20 micrometers did not alter the overall pattern, but the anodic reaction was restricted to a smaller region as shown in Fig. 5. The pH at the center of the disk for bulk pH 4 and 10 was changed by only a negligible amount since the bulk solution acidity or alkalinity dominated the behavior and buffered any shift from neutrality.

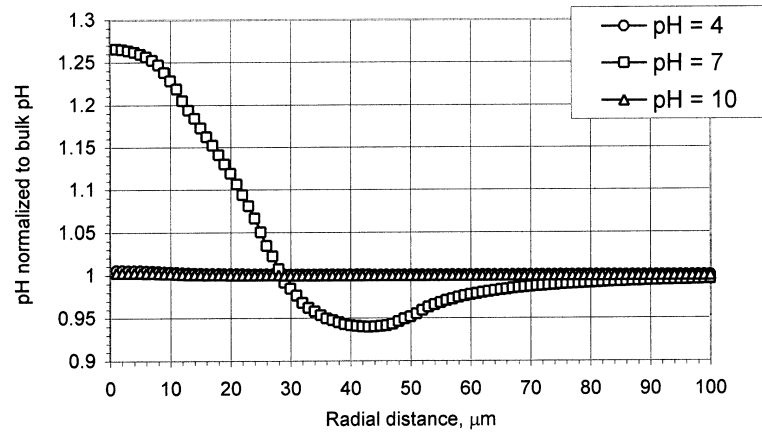


Fig. 3. Radial profile of normalize pH (pH/bulk pH) at 1 μm above the surface for different bulk pH (profiles evaluated for 50 μm anode radius)

The effect of vertical height from the disk-ring surface on the pH profile is shown in Fig. 4 for 50 μm anode radius. The pH profile at 0.1 and 1 μm were similar and pH changes were almost confined within a distance of 50 μm from the surface. Similar pattern was found for other anode disk radius. This finding is an important result to estimate an equivalent to the pH diffusion layer in stagnant electrolytes which can be useful in scale formation investigations in stagnant or quite solutions. Also, analytical techniques to measure pH changes during galvanic corrosion reactions can utilize such results [5]. Vertical pH profile, along the z-axis is also shown in Fig. 4. The vertical pH profile indicated a decrease in the pH values and bulk pH values were reached at around 50 μm . This observation justifies the selection of the total domain area which was 20 times the disk radius, i.e. 200 μm without forcing the bulk conditions on the solution.

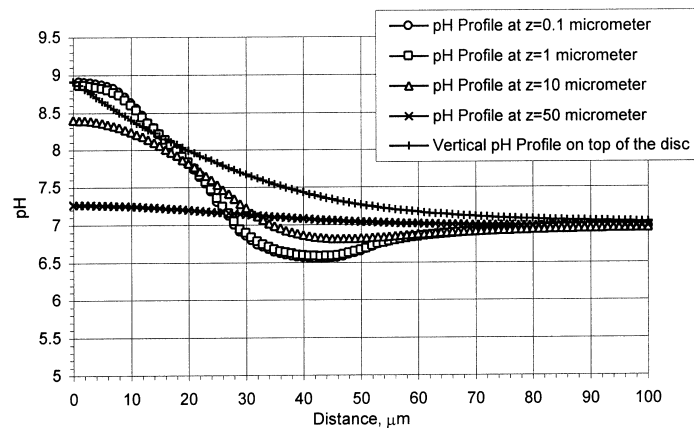


Fig. 4. Profiles of pH as function of height above the surface for 50 μm anode radius.

The effect of the anode radius on pH distribution is shown in Fig. 5 for bulk pH 7. In all cases the pH changes were confined to the anode radius and sharp pH changes were observed for 20 μm anode radius. An important result can be seen from Fig. 5 which was the pH transition from the cathode to the anode. This transition was smooth and alkaline conditions persisted on the anode annulus from the cathode side especially for large radius. This result provides an important indication of the local pH in relation with the anode geometry. For example, the pH was decreased below the bulk pH at almost half the anode distance and acidic conditions prevailed at the outer region of the anode.

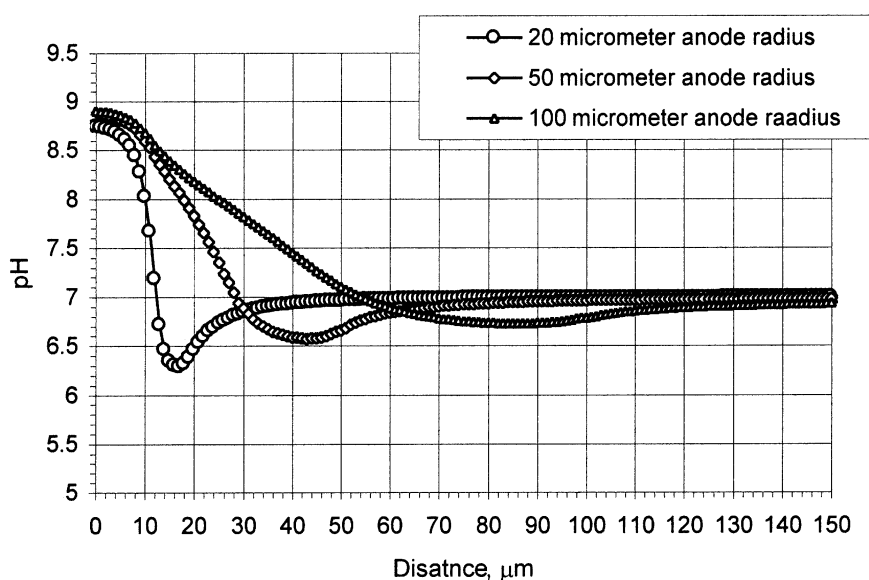


Fig. 5. Profile of pH at 1 μm above the surface for three different anodic plane radii, 10 μm , 50 μm and 100 μm .

In acidic electrolytes, iron surface does not passivate and ferrous ions dissolve into the solution. Fig. 6 shows the effect of the vertical distance on the concentration profile of ferrous ions for 50 μm anode radius. Sharp changes in ferrous ions concentration were observed at close distance to the surface; $<50 \mu\text{m}$. The concentration distribution extended beyond the anode radius into the inert plane. The vertical profile of ferrous ions concentration is also shown in Fig. 6. The ferrous ion concentration over the surface can be used to investigate the solubility limit and to understand the precipitation over the anode and passive film formation as function of local pH (Fig. 3).

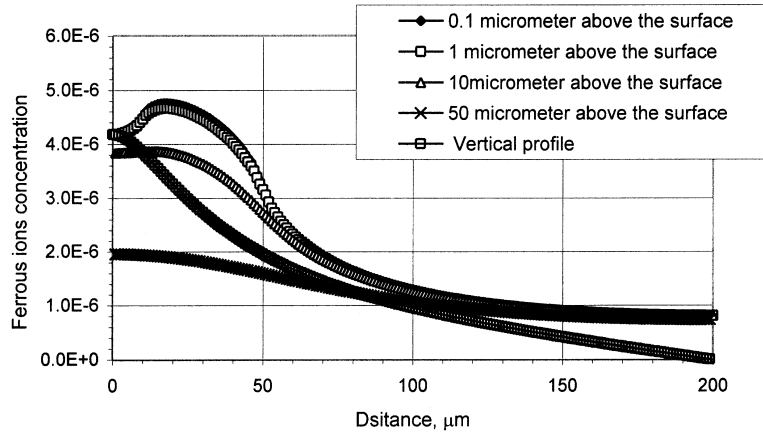


Fig. 6. Profile of ferrous ion concentration at different distances from the surface and vertical ferrous ion concentration profile at the center of the disk for 50 μm anode radius.

Effect of anode radius on the concentration profile of the ferrous ions is shown in Fig. 7 at 1 μm above the surface. Sharp variations in the ferrous ion concentration was observed for small anode radius, 10 μm . The ferrous ion concentration on top of the cathode was decreased as the anode radius was increased, unlike pH variations in Fig. 5. This can be attributed to the fact that cathodic reaction on the disk was the driving reaction for the corrosion system and the ferrous ion dissolution reaction resulted through electroneutrality conditions. Therefore, as the anode area was increased the concentration level of ferrous ions was decreased accordingly. One can predict that for small anodes, higher metal ions concentration prevails on the surface which may lead to film formation, due to precipitation limits. This may result in changing the corrosion system controlling step or reaction, e.g diffusion through the passive film. This fact can explain previous work observations [6] about utilizing fluorescent dyes to locate pH variations on the surface. It was observed that small inclusions had no fluorescent signal unlike large inclusions.

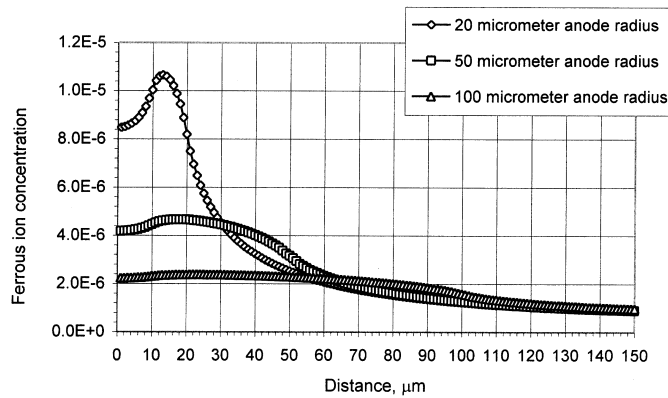


Fig. 7. Ferrous ion concentration profiles for different geometries at 1 μm above the surface.

Conclusions

The software used for this study provided a rapid, reliable vehicle to study reaction distributions on heterogeneous surfaces. The system can have more than one variable with nonlinear partial differential equations.

Most significant conclusions from this study can be summarized in the following:

1. Changes in pH over the cathode and the anode is a strong function of the bulk pH and the change was the highest for neutral bulk conditions. This important finding is attributed to the buffering action of water and can be only studied by including the ionization reaction of water, reaction (1), as homogeneous source or sink of H^+ and OH^- ions.
2. Most pH changes were confined to an equivalent pH diffusion layer in stagnant solution of 50 μm for pH 7 and 10 μm cathode disk radius. For other values of pH the pH diffusion layer is even smaller and change is confined to distance near the surface.

Acknowledgement. The author acknowledges the support of the College of Engineering Research Center, Department of Chemical Engineering at King Saud University, and Saudi Basic Industries Corporation (SABIC) for providing the main finite element software and support.

References

- [1] Fontana, M. *Corrosion Engineering*, 3rd ed. McGraw-Hill, 1986.
- [2] Jones, D. *Principles and Prevention of Corrosion*, 2nd ed., New York: Prentice Hall, 1996.
- [3] Brett, C.M.A. and Brett, A.M.O. *Electrochemistry: Principles, Methods, and Applications*. New York: Oxford University Press, 1993.
- [4] Rynders, R.M., Palk, C.H., Ke, R. and Alkire, R.C. *J. Electrochem. Soc.*, 141, No. 1439 (1994). Alkire, et.al., and J. Electrochem. Soc., 143, No. L174, (1996)
- [5] Alodan, M. and Smyrl, W.H. *J. Electrochem. Soc.*, 144, No. L282 (1997).
- [6] Alodan, M. 9th Middle East conference on Corrosion, NACE, Bahrain, 2001.
- [7] Alodan, M. and Smyrl, W.H. *J. Electrochem. Soc.*, 145, No. 5 (1998).
- [8] Pillay, B. and Newman, J. *J. Electrochem. Soc.*, 140, No. 2 (1993).
- [9] Morris, R. and Smyrl, W. *J. Electrochem. Soc.* 136, No. 11 1989.
- [10] A. Abu-Khalaf, A. Soliman, M. and El-Dahshan, M. *J. King. Saud Univ.*, Vol. 8, Eng. Sci. pp 71, 1996.
- [11] Geankoplis, C.J. *Transport Processes and Unit Operations*, 3rd ed., Encylewood Cliffs, NJ: Prentice-Hall, 1993.
- [12] Alodan, M. and Smyrl, W. *Proceeding Volume PV97-26, Electrochemical Society Conference*, Paris, 1997.
- [13] Fleischmann, M. Pons, S., Rollson, D.R. and Schmidt, P.P. *Ultramicroelectrodes*, Datatech Science Publishers, 1987.
- [14] Newman, J. *Electrochemical Systems*, 2nd ed., Englewood Cliffs, NJ: Prentice Hall, 1994.
- [15] Cussler, E. *Diffusion, Mass Transfer in Fluid Systems*, New York: Cambridge University Press, 1984.
- [16] R. Fiedler, R. Hazcdon, T., Schnelle, T. Richter, E., Wagner, B. and Fahr, G. *Anal. Chem.*, 61, No. 820 (1995).

نمذجة تغير تركيز أيونات الهيدروجين فوق مواقع التآكل

ماهر بن عبدالله العودان

قسم الهندسة الكيميائية ، جامعة الملك سعود
ص. ب. ٨٠٠ ، الرياض ١١٤٢١ ، المملكة العربية السعودية

(استلم في ٠٧/٠٧/٢٠٠١م، وقبل للنشر في ٠٣/١١/٢٠٠١م)

ملخص البحث. تمت دراسة تفاعلات مختلفة للتآكل و تأثير تركيز أيونات الهيدروجين على نواتج التفاعل. كما تم نمذجة تراكيز ايونات الهيدروجين و أيونات الحديد مع أخذ في الاعتبار تفاعل التأين للماء كتفاعل متجانس في المحلول المحيط لموقع التآكل. كذلك تم محاكاة مواقع التآكل لسبائك الحديد و الالومنيوم بوجود المترسبات شبه المعدنية في تلك السبائك. تشير نتائج النمذجة الى ارتفاع الرقم الهيدروجيني عند مواقع اختزال الاوكسجين و المتغير على حسب البعد من موقع التآكل و الرقم الهيدروجيني للمحلول المحيط.